LJMU Research Online

Yu, Q, Liu, K, Yang, Z, Wang, H and Yang, Z

Geometrical risk evaluation of the collisions between ships and offshore installations using rule-based Bayesian reasoning

http://researchonline.ljmu.ac.uk/id/eprint/14875/

Article

For more information please contact researchonline@ljmu.ac.uk

Geometrical Risk Evaluation of the Collisions between Ships and Offshore Installations using Rule-based Bayesian Reasoning

Qing Yu[&], Kezhong Liu[&], Zhisen Yang, Hongbo Wang and Zaili Yang[*]

Abstract: Increasing human installations and vessel traffic in offshore waters render a collision risk between ships and offshore installations (SOI). Past decades have witnessed many accidents occurred in the offshore waters involving complex traffic networks. To safeguard offshore installations and improve water-bound transport safety, this paper proposes a novel Bayesian-based model to assess the SOI collision risk involving passing ships. It first identifies the relevant risk factors with the aid of a geometrical analysis concerning SOI collisions. The causal relationships between the risk factors are numerically defined by causal rules with a degree of belief structure, while a Bayesian network (BN) is constructed to aggregate the evaluated value of each risk factor and to assess the collision risks involving different navigational environments. To illustrate the new model, a real case on SOI collision risk in the Liverpool Burbo Bank offshore wind farm is investigated. The results provide empirical evidence for SOI collision risk analysis under complex water conditions and uncertain navigational environments and hence useful insights on SOI collision avoidance.

Keywords: Maritime risk, ship collisions, geometrical evaluation, Bayesian network

1. Introduction

The past decades have witnessed an increasing number of human installations (e.g., oil & gas platforms, wind and tide farms) in offshore areas to meet the continuous demand for energy. Meanwhile, shipping traffic becomes much intensive due to fast-growing sea transportation in the same areas. As a result, it causes a high concern on collision risks between ships and offshore installations (SOI), evidenced by accidents such as the SOI collision in the Arabian Sea in 2005 (Daley 2013). In this accident, an offshore oil platform was totally damaged because of the collision with a multipurpose support vessel, resulting in an oil leak and 22 casualties (Daley, 2013). A report by OGP (2010) reveals the passing ships cause one accident every 2 years on average, and nearly 52% of SOI collisions accidents lead to significant, severe

---

[&] The first two authors contributed equally to this work and should be considered co-first authors.
[*] Corresponding Author.
E-mail Address: Z.Yang@ljmu.ac.uk (Z. Yang).

or total losses[1]. Referring to current studies and reports (Dai et al., 2013), the importance of SOI collision has been emphasized in the literature and practice. It is well noted that the constraints of these reports are to highlight the severity of SOI collision risk, not a specific illustration between different types ships (service/passing) and offshore collisions (wind farms/oil platform) (Ma et al., 2020). To safeguard the offshore waters, UK maritime and coastguard agency published MGN 543 Offshore Renewable Energy Installations Safety Response guidance (Maritime and coastguard agency., 2016.), which suggested that 'these should evaluate all navigational possibilities, which could be reasonably foreseeable, by which the siting, construction, extension, operation and de-commissioning of an OREI could cause or contribute to obstruction of, or danger to, navigation or marine emergency response. They should also be used to assess possible changes to traffic patterns and the most favorable options to be adopted, including those of operational site monitoring'. Guidance on strengthening maritime safety supervision of offshore wind farms (China Maritime Safety Administration) emphasised that the risk of a collision between a ship and an offshore wind farm should be fully awared, any new project need to be assessed before construction to reduce the maritime risk in offshore waters. EU MSP also highlighted that 'maritime transport and offshore wind can come into conflict when new offshore wind farms are to be built or existing ones expanded – e.g. into areas where shipping activity is intense'.

Constructing offshore installations to withstand the SOI collisions is extremely extravagant if the risk cannot be appropriately addressed. However, the state of the art studies relevant to SOI collisions presents the collision risk from a traffic flow perspective (Yu et al., 2020b) which often ignores the characteristics of individual passing ships and is incapable of modelling SOI from a micro-level for effective collision avoidance in real-time situations.

A number of collision avoidance methods and support systems have been proposed for the purpose of assessing collisions between ships, developing decision support systems or establishing collision simulation platforms (Gil et al., 2020a). In line with developments in the collision alert system, several geometric collision assessment approaches are applied, such as relevant distance approach (i.e. distance at closest point approach (DCPA) and time to closest point approach (TCPA)), Minimum Distance to Collision approaches (Gil et al., 2020b), ship

---

[1] The pure SOI accidents are scanty given many offshore installations are new. The Mumbai high north incident—collision with the vessel MV Samudra Suraksha, 2005 and the Collision accident between supply vessel MV Celeste Ann, 2013 are used here to demonstrate that that SOI collision risk could cause a catastrophic consequence as the existing similarity between them.

domain approaches (Ozturk et al., 2019), velocity obstacle avoidance approaches (Huang et al., 2019) and obstacle zone by target based approaches (Kayano and Kumagai, 2017). The collision can be dynamically evaluated when updating the system with ship real-time navigation data. These geometrical approaches are incorporated with other aggregation approaches (e.g. liner aggregation algorithms, fuzzy logic, Bayesian networks) in some studies to obtain an integrated risk value. However, in the SOI field, relevant research focuses on risk assessments (e.g Mehdi et al., 2019) and collision decision support systems are rare. In the meantime, most of the used methods are not capable of providing real-time risk value evaluation, lacking adequate input data specific to the offshore installation (Mehdi et al., 2018). It is therefore very crucial to develop a new risk model aiming to evaluate the risk of a single ship collision under a dynamic and complex environment.

The aim of this study is to develop a risk analysis model to aid the anti-collision decision of a ship passing offshore installations, while to aid local Vessel Traffic Service (VTS) to dynamically evaluate individual SOI risks of each passing ship in the controlled waters. In the model, a causation rule-based Bayesian network (BN) will be applied to evaluate SOI collision risk using objective data (i.e. AIS data, weather reports). Firstly, the relevant risk factors for risk model construction are identified from ship navigational variables (e.g. speed, course) and natural environment parameters (e.g. wind, current). Secondly, the interrelationships and interdependencies among the risk factors and the SOI collision risk are defined through the development of causal rules. Thirdly, a BN is established to evaluate the SOI collision risk by aggregating every piece of risk information from all risk factors. At last, the proposed model is validated and compared with an established collision model to demonstrate the reliability and feasibility of the new model.

This rest of the paper is organised as follows. Section 2 reviews the current studies in ship collision risk modelling. The SOI collision risk model is presented in Section 3. To test the feasibility of the new risk model, this study investigates a real case on the SOI collision risk in the waters near the Liverpool Burbo Bank Offshore Wind Farm in Section 4. In Section 5, the assessment results are compared with the one from an established risk model to verify the robustness of the new model. Based on the comparative analysis, the superiorities and the limitations of the new model over existing methods are discussed for demonstrating its implications. Finally, conclusions are drawn in Section 6.

2. Literature review

Previous studies involve a wide variety of modelling approaches from different views to evaluate ship collision risks under different navigation situations. To ensure the rationality of the new SOI collision model, this section reviews the state-of-art collision risk models in the maritime sector to illustrate their strengths and weaknesses in applications.

2.1 Geometric collision models

Geometric collision models address the spatial-temporal relationships between ships and collision objectives (e.g. ships, installations), including two mainstream approaches: synthetic indicator approach (SIAs) and safe boundary approach (SBAs) (Chen et al, 2019).

SIAs consider own ship and collision obstacles as mass points and discuss the collision risk under an assumption that if the objects (i.e. ships/installations) remain their status and motions, how far (i.e. DCPA) and how long (i.e. TCPA) an obstacle ship will pass their closest point. They describe the spatiotemporal relationship between ship-ship/ship-installation via dynamic indicators such as relative distance, relative speed, relative direction and heading. The collision risk under dynamic situations can be evaluated by illustrating collision functions in the studies by Wang et al., (2013) and Zhang et al., (2016). As results, a numerical risk value can be obtained to show the risk level of an encountering situation. Zhang et al (2015) developed a ship encounter risk model, in which CPA, relative distance/direction and speed were selected as the key parameters to model multi-ship collision risk. In his study, a four-ship-encounter situation was simulated to provide the best collision avoidance decision making based on International Regulations for Preventing Collision at Sea (1972). Similarly, Wang et al (2017) involved TCPA and DCPA to analyse ship collision under close-quarters situations, in which a four-stages-collision-avoidance-procedure was established. Currently, SIA is attracting growing attention in unmanned ship collision avoidance, as illustrated by recent relevant papers (e.g. Woo and Kim, 2020; Cho et al., 2019; Wang et al., 2020 and Shen et al., 2019).

SBAs use a concept of safe boundaries to evaluate collision risk and suggest the risk is likely to happen if a ship's safe boundaries are violated by other ships/installations. It should be noted that the dimensions of setting ship domains are associated with the selection of safety criteria under different collision situations. Therefore, in addition to the indicators used in SIAs, SBAs cover other factors such as ship size, blind areas and ship manoeuvrability that affect the ship's safe boundaries. In SBAs, collision risk is obtained by calculating the overlapping areas between two ships' safe boundaries. An original way of calculating a ship safe boundary

dimensions is to multiply the ship size with a constant value. For instance, Coldwell (1983) suggested the fore sector of a ship's boundary under an overtaking situation should be the range between 1.75 times (minimum) to 6 times (maximum) ship length. This crude definition could lead to the misconduct of ship behaviour or ignorance of the effect of other impact factors. The constant ship boundary is therefore lately updated by empirical ship domain (Hansen et al., 2013), knowledge-based ship domain (Zhu et al., 2001) and analysis-based ship domain (Wang et al., 2010). Applications of SBAs can be found in many studies including Fiskin et al., (2020), Im and Luong, (2019), Zhang and Meng, (2019), and Szlapczynski et al., (2018).

Although the two geometric approaches address the collision risk from different views, important risk variables such as relative distance, relative angle and speed are within the consideration of both of them. SIAs are used to describe the collision risk when ships' dynamic data is available, while SBAs are preferable in situations where safe boundaries can be defined.

2.2 Causation collision models

Evaluation of maritime risk based on causation models is challenging given that maritime environment is complex, involving a large number of internal/external influencing factors (e.g. machine failure, human error, natural environment, ship monitoring and management).

When risk assessment approaches (e.g. fault tree analysis, event tree analysis to assess maritime risk) are applied in causation models, the impact magnitudes of factors can be described by numerical values. Generally, expert judgment and experience are the major way to derive such numerical values because it is difficult to obtain the values directly from objective data soures (Yu et al., 2020b). Thus, belief degrees and linguistic states are used to reflect experts' psychology and behaviours. One of the realistic approaches used to model discrete linguistic terms in maritime risk analysis is fuzzy logic analysis (FLA) (Ozturk and Cicek, 2019). For example, Goerlandt et al. (2015) used an FLA to model uncertain data in ship traffic parameters and aggregate their membership degrees to evaluate mutual ship collision risk. Perera (2011) applied an FLA to develop a collision avoidance intelligent decision-making system, based on collision distance, collision region, relative speed, relative angle, course and speed change. Despite showing some attractiveness, the applications of FLA in maritime risk modelling reveal some practical shortcomings: 1) it is often time costly to aggregate data; 2) FLA fails to provide bi-directional diagnosis and simulation; 3) it is difficult to conduct sensitivity analysis, and 4) FLA can cause the missing of useful information during modelling processes.

BNs for modelling randomness in data and evidential reasoning (ERs) for incompleteness are combined with FLA to address the abovementioned shortcomings. They are both widely used with FLAs to aggregate discrete data, yet recently BNs are more preferable because of its capability of bi-diagnosis analysis, scenario simulations, description of interrelationships between risk factors, and sensitivity analysis to mathematically unsophisticated users. For instance, Yang et al. (2008) pioneered a rule-based Bayesian reasoning approach to prioritise system failures, and it was applied in different maritime risk analysis such as offshore engineering safety system (Yang and Wang, 2015), human reliability onboard oil tankers (Zhou et al., 2018) and maritime supply chain risk (Wan et al., 2019). However, uses of rule-based Bayesian reasoning in collision-related areas are new, few collision models from generic views can be found in previous studies (e.g. Perera et al., 2012; Ung, 2019) and fewer on the analysis the single ship collision from the geometric point of view.

2.3 SOI collision models

In SOI collision risk analysis, most of them are undertaken from a macroscopical viewpoint. These studies are conducted to identify the influential factors related to SOI collisions and to discuss the collision risk by considering the factors such as navigation environments, traffic flow conditions, machine failures and human error. For example, Yu and Liu (2019) applied a subject risk model to assess the vessel collision risk near offshore installations using a hybrid approach. The study collected expert judgements to develop a BN model and further analysed the collision risk for different ship types. As results, the study concluded the fishing vessels have the highest collision probabilities in the study waters, while the consequence of oil tankers collision is catastrophic.

From a macroscopical perspective, previous studies started with the mapping of traffic pattern in waters to compare the traffic characteristics under the impacts of installations (Martin et al., 2016, Yu et al., 2020a), then developed a risk model to assess the risk. The Pederson collision model is the most widely used when it comes to the analysis focusing on collision probability (e.g. COLLIDE (Safetec, 2002), COLWT (Otto, 2004), MARIN (SAFESHIP, 2005)). In the Pederson model, geometrical analysis is supplemented to calculate numbers of collision candidates and causation probabilities are obtained from experience. For example, Daniel (2006) analysed the collision risk between ships and offshore structures. The study introduced two types of collisions, which were associated with powered ship and drifting ship collisions, respectively. The model used in this study called COLWT, which analysed the powered ship

collision risk based on the Pederson model. Martin et al. (2015) studied collision risk in the North sea and Norwegian sea. To adopt the COLLIDE risk model in arctic conditions, the authors proposed a holistic approach based on the hybrid of fault tree and Bayesian networks to analyse the interrelationships between risk variables. Mujeeb-Ahmed et al. (2019) applied the Pedersen collision model to assess SOI collision in Korean waters. In their study, collision candidates were obtained from AIS data and causation probabilities were acquired from previous studies. The collision probability was linearly calculated by combining geometrical indicators (i.e. number of collision candidates) with causation probabilities. Similarly, Yu et al. (2018) evaluated the collision risk in offshore wind farms (OWFs) water. Although the Pederson model is widely used in previous studies, its applications still reveal a high level uncertainties   as its causation factors are numerically defined with generic values, which are difficult to acquire and inaccurate to describe the factors' impact magnitudes. Moreover, this model investigates the SOI collision from a traffic flow level under a static situation, which fails to model the dynamic evaluation of the collision risk of a single ship.

Currently, some new approaches are applied to analyse the SOI collision risk. For example, Yu et al. (2020b) proposed a multiple-data driven risk model for SOI collision. In the model, an unsupervised machine learning approach was applied to train BNs from AIS data, then the expert judgements were adopted into the model to assess the ship traffic collision risk. Martin et al (2020) presented a new risk model for the evaluation of SOI collision to replace the industry-standard COLLIDE risk model. In the study, the author claimed that the new model was more transparent and was capable of providing a clear understanding of the mechanisms among risk factors in SOI collisions.

In contrast with the macroscopical viewpoint, the microscopical studies related to SOI collision are relevatively scanty. An example can be found in a model proposed by Wu et al (2019). Aid with FLAs, the study attempted to develop a geometrical model to enable a ship-fixed installations collision model. In the model, linguistic states were assigned to variables and fuzzy membership functions were proposed to obtain belief degrees, then an FLA approach was used to aggregate all pieces of information into the final risk values. Although the model showed attractiveness, the aforementioned shortcomings of FLAs (in Section 2.2) restricted its applications in practice.

3. Developing a rule-based BN model for SOI collision risk analysis

This section describes the development of a novel SOI collision model by using a rule-based BN. The first step is to identify the SOI collision-related risk factors with the aid from a geometrical analysis. In the second step, data/information used to describe the risk factors from both objective and subjective sources is transformed and expressed by the predefined grades with a belief degree structure. In the third step, sets of causation rules are developed to define the relationships between the risk factors and SOI collision risk levels. Finally, a BN is used to model the established rules and to conduct the risk inference.

3.1 Identifying the SOI collision risk factors

The identified SOI collision risk factors are selected from two aspects: navigational conditions and natural environments, which are two major areas influencing SOI collision. Other aspects such as human reliability, technical failures and traffic management are excluded in the current model. It is because that: on the one hand, vessels often pass an installation in a short period, compared to the investigated variables, these variables (e.g. human error and facility performance) are relatively stable and their impacts are not as significant as the investigated ones; on the other hand, in this paper, we referred to the similar studies in the literature on ship collision risks, in which such variables as human and machinery failures were not taken into account (Khan et al., 2020). The detailed information of identified risk factors is presented as follows.

3.1.1 Navigational conditions

Figure 1 presents a classical SOI collision risk by illustrating the navigational condition of ships passing an offshore installation. Assuming there are a number of offshore structures located in the water area that is close to a shipping route, the boundaries of the structures along the shipping traffic flow side (left side) is l nautical miles; a ship passes the waters at speed V in which its position is set as the origin point of coordinates. The X coordinate is along the true north direction and Y coordinate follows the east direction. According to the defined coordinates, the distance D between the ship and the nearby offshore structures is defined as a horizontal distance D_h that is along the X coordinate and a vertical distance D_v that is along the Y coordinate.
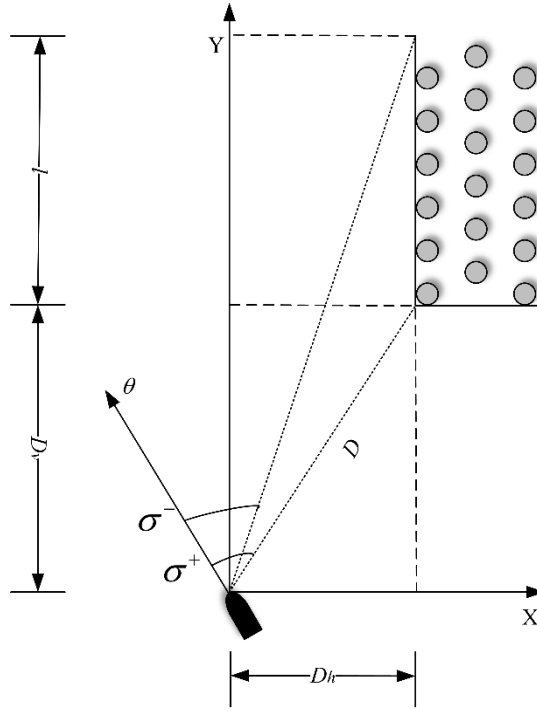
Figure 1: A ship passing an area of offshore installations

Let the ship heading be θ, the relative angular direction measured from a ship heading to offshore structures is defined as the relative bearing σ. A group of offshore installations has a far point relative bearing in Equation 1

$$\sigma^- = arctan\left(\frac{D_h}{D_v + l} - tan\,\theta\right) \times \frac{180^\circ}{\pi}$$

(1)

and a near point bearing as Equation 2

$$\sigma^+ = arctan\left(\frac{D_h}{D_v} - tan\,\theta\right) \times \frac{180^\circ}{\pi}$$

(2)

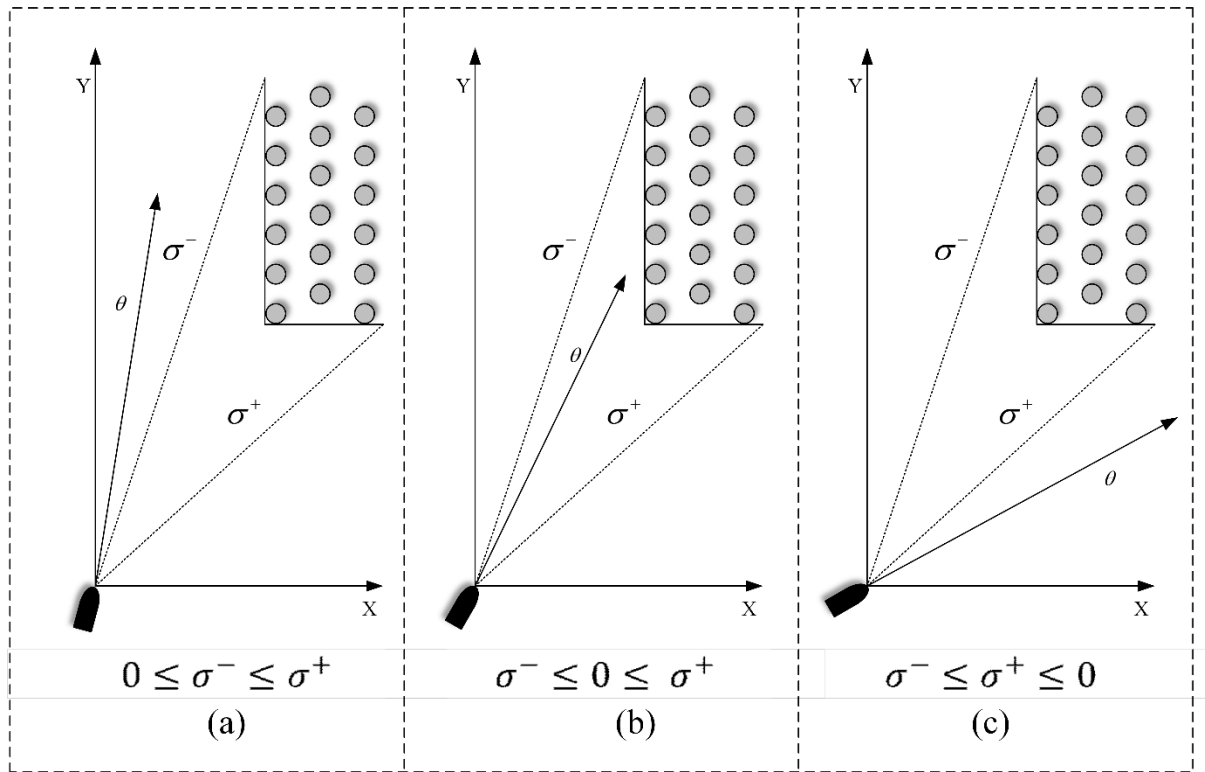Figure 2: Ships passing with different headings

We define three risk factors relating to the navigational conditions to assess collision risk, including the passing distance D, the relative bearing of structure σ (contains σ^- and σ^+) and the ship speed V. Assuming that if $D \leq 0$, a collision occurs. For the σ, when $\sigma^- \leq 0 \leq \sigma^+$ (Figure 2b), the ship will collide the structure if there are no changes on its course; if $0 \leq \sigma^- \leq \sigma^+$ (Figure 2a) or $\sigma^- \leq \sigma^+ \leq 0$ (Figure 2c), the ship could pass the installation. For the V, if V is higher than an average speed (the average speed of all ships passing waters, it can be obtained from statistical analysis of traffic flow data), the collision risk is increased.

In addition of the aforementioned geometrical parameters, risk differences on ship types are emphasised in previous research studies (e.g. Yu et al., 2020a; Dai et al., 2013; Presencia and Shafiee, 2018) so they have been included in the SOI collision model.

3.1.2 Natural environments

The risk factors associated with natural environments are selected based on the previous SOI collision studies via a thorough reivew (see Table 1).

Table 1 Key natural environment selection

Reference	Inputted data	Factors

		Visibility	Day/night condition	Wind	Sea state	Water density	Temperature
Balmat et al., 2009	Weather records	✓	✓	✓	✓		
Balmat et al., 2011	Weather records	✓	✓	✓	✓		
Burmeister et al., 2015	Real-time weather data	✓		✓	✓		
Goerlandt et al., 2017	Accident records		✓	✓	✓		
Hegde et al., 2018	Background knowledge	✓			✓	✓	
Luo and Shin, 2019	Literature review	✓		✓	✓		
Wu et al., 2019	Background knowledge	✓	✓	✓	✓		
Ozturk and Cicek, 2019	Literature review	✓	✓	✓	✓		
Fan et al., 2020	Literature review	✓	✓	✓	✓		✓
Utne et al., 2020	Real-time weather data	✓	☐	✓	✓		

For instance, Utne et al (2020) selected visual conditions and weather conditions (wind and sea state) that impact ships to maintain a safe distance to obstacles as inputs; Luo and Shin (2019) reviewed the studies related to maritime accidents to provide evidence that the natural environment factors (i.e. wind, wave and visual condition) are important in maritime accident research fields; Burmeister et al (2015) discussed the collision avoidance and operation measures under harsh weather conditions, and concluded that the poor visibility, heavy weather condition and darkness significantly impact the ship' collision avoidance behaviour. In the SOI collision studies, Wu et al. (2019) suggested four natural main variables that are wind speed (W), sea state (S), visibility (Vis) and day/night time (D/N) to evaluate ship and bridge collision risk.

Within the context of SOI in this paper, the *wind speed* is significant as the wind could cause a shift of ship position and heavily affects ship manoeuvring in waters near offshore installations. At sea, wind speed is described by the Beaufort wind scale. The *sea state* is deemed as a crucial risk factor in many ship collision risk analysis studies. In the scenarios where ships face rough sea conditions (e.g. Mumbai High North Platform Disaster (Daley, 2013)), it is very difficult to control and maintain the ships' courses. The sea states are often defined using the Douglas sea scale by current speeds. Poor *visibility* contributes to high

collision risk because it interferes with ship overwatches. Visibility less than 2 nm is considered as poor visibility in navigation and ships should take a stricter overwatch to avoid collisions. If the visibility is less than 0.5 nm, then the overwatch with eyes is almost impossible. The *day/night time* also affects visual overwatches. Poor lighting and marking will decrease the chance of the offshore structures being observed, thus increasing the SOI collision risk. Previous studies of a ship collision risk analysis claimed that approximately 67% ship and bridge collision accidents happened in nights (Wu et al., 2019). Taking into account all the identified key natural environmental factors influencing ship collisions, four factors including wind speed, sea state, visibility and day/night are chosen in this work.

3.2 Assigning linguistic states to the risk factors

Four graded linguistic states of 'low', 'medium', 'high' and 'very high' are assigned to the above-identified risk factors in Sections 3.1.1 and 3.1.2 except day/night and ship type to rank their influential magnitudes to SOI collision. The risk factor of day/night time only has three states, the daytime is defined as the 'low' risk state, the night-time is defined as the 'medium' state and the twilight is defined as the high-risk state. This is because the dark environment and fatigue in the night-time have an effect on the on-board overwatch.

The risk factors are, based on their features, firstly grouped into two categories of navigation conditions (*NC*) and natural environments (*NE*). Then, numerical definitions are assigned to each risk factor, in which thresholds are used to represent the risk grades. The thresholds are referred from the previous studies and further verification of their use in this study. It is described in the ensuing section. As a result, detailed information about the categories and the numerical definitions of linguistic states are presented in Table 2.

Table 2 Thresholds assignment for linguistic states of the SOI risk factors

Risk factors	Threshold values			
	Low (L)	Medium (M)	High (H)	Very high (VH)
Navigation Conditions				
Passing distance (nm*)	3.5	2	1	0.5
Speed (knots)	3	5	10	16
Relative Bearing (degree)	±180	± 90	±45	± 22.5
Ship type	Service ship	Others	Ferries	Oil and Gas tankers

Natural Environments				
Sea state (Douglas scale)	1	3	5	7
Wind (Beaufort scale)	2	3.5	5	6
Visibility(nm)	5	3	1	0.5
Day/Night	Day	Night	Twilight	-

*nm: nautical miles

(1) **Ship type:** Four ship categories are used to divide the passing ship in offshore waters based on their severity of consequence. There are ranked as service ship, others (e.g. container, bulkers, general cargo ship), ferries and oil and gas tankers (Dai et al., 2013; Presencia and Shafiee, 2018)

(2) **Passing distance:** According to the two widely accepted safety recommendations of MGN 543 (2016) Offshore Renewable Energy Installations Safety Response and MGN 371 (replaced by MGN 543) from the UK maritime agency, different risk levels can be defined depending on a ship passing distance. The recommendations suggest that ships passing offshore installations with a distance less than 0.5 nm are intolerable indicating very high risk; a passing distance between 0.5 nm and 3.5 nm are tolerable if as low as reasonably practicable (ALARP). Specifically, a distance between 0.5 nm and 1 nm and between 1 nm and 2nm are assoicatd with high and medium risk, respectively. Furthermore, ships passing the installations with a distance larger than 3.5nm are broadly acceptable (i.e. low risk).

(3) **Speed:** The grades for speed refer to historical AIS data. In a statistical analysis, Yu et. al., (2020) collected two-year AIS data (before/after installations) and characterised the ship traffic flows in the vicinity of OWFs. The obtained results show that the majority of the ship speeds are between 5 knots and 10 knots; ship speeds less than 5 knots are low; speeds from 10 knots to 16 knots are high and speeds higher than 16 knots are very high.

(4) **Relative Bearing:** the grades representing the risk of collision candidates (e.g. fixed structures, ships) under different bearings are based on COLREGs[2] and common practices on board ships (Tam and Bucknall 2010; Goerlandt et al., 2015). Normally, a collision candidate in front of a ship with a relative angular direction between 22.5° port board side and 22.5°

---

[2] International Regulations for Preventing Collisions at Sea (COLREGs)

starboard side is very high risk; the candidate's bearings between 22.5° and 45° on both sides are risky, between 45° and 90° are medium risk and over 90° is low risk.

(5) **Wind, Sea, Visibility:** Referring to local best practice and common knowledge (Goerlandt et al., 2017; Baksh et al., 2018), calm sea state (Douglas sea Scale less than 1), calm wind speed (Beaufort scale less than 2) and visibility larger than 5 nm are defined as low risk; the choppy sea (Douglas sea Scale of 3), breeze wind (Beaufort scale of 3.5) and good visibility (large than 3 nm) are medium risk; rough sea (Douglas sea Scale of 5), fresh breeze wind (Beaufort scale of 5) and low visibility (0.5-1 nm) are at a high-risk situation; and very rough sea (Douglas sea Scale higher than 7), strong wind (Beaufort scale higher than 6) and poor visibility (less than 0.5 nm) are at a very high-risk situation.

(6) **Day/night time:** previous studies have shown a great interaction between time and accidents as the light conditions changes as many accidents occurred during twilight and night (Goerlandt et al., 2017). Therefore, this study states the time with three states as day, twilight and night time. The lengths of each time are related to the sun position, which is changing in different season and position. For instance, nautical twilight is defined when the sun is less than 12° below the horizon. The detailed information of the day/twilight/night time can be checked from the local sun graph.

3.3 Data discretisation.

In general, the observations of the above-mentioned risk factors are presented by single values, which cannot be directly used in BNs without appropriate raw data transformation. To convert the collected raw data into the degree of belongs to the defined states, the following functions are used.

Assuming factor X has a set of k states $(S_1, S_2, \cdots S_k)$, the assigned threshold values for the states are $(TH_1, TH_2, \cdots TH_k)$, when an observation value y falling in an interval (TH_m, TH_{m+1}) $(m \in k)$, the belonging degree BD of this observation on states S_m and S_{m+1} can be therefore calculated by using the following functions:

$$BD_{S_m} = 1 - \frac{y - TH_m}{TH_{m+1} - TH_m}$$

(3)

$$BD_{S_{m+1}} = \frac{y - TH_m}{TH_{m+1} - TH_m}$$

(4)

For instance, based on Table 2, threshold values assigned to *Vis* are $(TH_L = 5\ nm, TH_M = 3\ nm, TH_H = 1\ nm, TH_{VH} = 0.5\ nm)$, an observation *Vis=1.4 nm* is between $TH_M = 3\ nm$ and $TH_H = 1\ nm$. Using Functions 3 and 4, $BD_M = 1 - \frac{1.4-3}{1-3} = 0.2$ and $BD_H = 0.8$, the observation can be presented as a set of belonging degree *{(0, L), (0.2, M), (0.8, H), (0, VH)}*.

3.4 Establishment of conditional probability tables (CPT)

A causation rule-based approach is applied to numerically describe the causality between all the eight risk factors and SOI collision risk level. In this approach, defined rule sets are used to convert p attendance attributes $\{A_1, A_2, ..., A_p\}$ into a consequence of q states $\{C_1, C_2, ..., C_q\}$ by assigning belonging degrees β_s $(s = 1,2 ..., q)$ to C_s $(s \in q)$. For example, a conventional rule can be expressed as:

$$\textbf{IF } A_1 \text{ and } A_2 \text{ and } ... \text{ and } A_p, \textbf{ THEN } \{(\beta_1, C_1), (\beta_2, C_2), ..., (\beta_q, C_q)\}.$$

where the cause part is a set of grades $A = \{A_1, A_2, ..., A_p\}$. Under this situation, a set of belonging degrees is assigned to the consequence part as $\{(\beta_1, C_1), (\beta_2, C_2), ..., (\beta_q, C_q)\}$ for the description of how each C_s $(s = 1,2 ..., q)$ is believed to be the result of β_s. β_s can be assigned with experience or by using an equivalent influential method (Yang et al., 2009).

In this study, influential magnitudes of the risk factors are expressed by three conditional probability tables (CPTs). Given a relatively small number of OWFs and the emerging SOI collision risk studies, the experts of good experience on navigational safety passing OWFs are available to a limited extent. Despite the authors' great effort, the size of the quailfiied experts is small, when they have to be very selective by taking into account their experience and knowledge to provide valuable data. Finally twelve experts participanted in this study. The panel of experts covers experienced staff members who are closely working in relative fields to ensure the quality of the obtained subjective database, including two officers from China Maritime Safety Administration, two officers from China Port and Shipping Administration, two managers from OWF maintenance companies, two captains from Orient Overseas Container Line or China COSCO shipping group, an surveyor from Lloyd's Register, an inspector from the UK Health and Safety Executive (HSE) and two experienced scholars from Norway and Portugal. The confidence of the data quality comes from the consistency among their judgements. Furthermore, the good result from the sensitivity analysis in the validation part proves the quality of the data from the experts.

A survey is designed to collect expert judgements. For example, the experts are asked: 'when a service ship passes an OWF in a distance of 3.5nm with low speed (less than 5 knots), while the relative bearing of the OWF is large than 135°, how risky the ship is?' and the experts all agree that the ship is 100% at very low collision risk. Based on this judgement, an IF-THEN rule is established: IF *ship type=service ship, relative bearing=low, passing distance =low and speed=low*, THEN *navigation condition = {1.0(low), 0(medium), 0 (high) and 0(very high)}*. Similarly, a total of 256 rules of navigation condition, 192 rules of environment condition and 16 rules of the final risk are established.

3.5 Developing a BN model for SOI

This section describes the conversion of the above causation rules into a BN structure. Total of 11 nodes is used in the BN, including 8 root nodes (i.e. RIFs), 2 intermediate nodes representing *NC* and *NE*, and the target node being SOI collision risk. More specifically, s*hip type, distance, relative bearing* and *speed* are four parent nodes of *NC*; *wind*, *sea state*, *visibility* and *time* are four parent nodes of *NE*, and the node of SOI collision risk is the child node of *NE* and *NC*. It should be noted that the BN structure related to *NC* and *NE* is verified by the data collected from AIS and weather report (the AIS data is one-year data of all the ships (trajectories) passing the waters near an OWF in China in 2017 (collected from China Maritime Safety Administration). The real-time data on the weather and sea states relating to each recorded ship in the AIS data is obtained from the National Meteorological Information Center, available at http://data.cma.cn). The analysis of AIS data used in the risk analysis reveals that no other connections among the nodes are of significant statistical relation. As a result, the BN structure is finalised and shown in Figure 3.
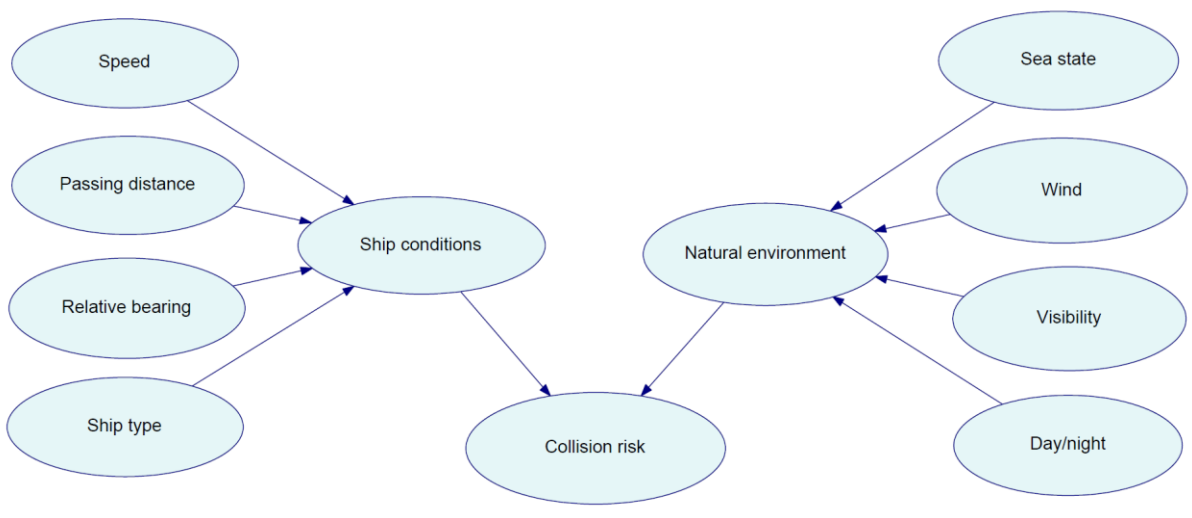
Figure 3: BN structure

Four states of *'low'*, *'medium'*, *'high'* and *'very high'* are assigned to two intermediate nodes and the final node to classify the SOI collision into different risk levels. Through inputting the developed CPTs into the BN structure, a generic BN model for the evaluation of the SOI collision risk is developed. It can aggregate the input data from the root nodes (i.e. RIFs) to produce a marginal probability on the final node (i.e. SOI collision risk) for risk analysis.

3.6 Risk prioritisation

To visualise and prioritise the risk analysis results from BN, a set of utility values U_k ($k \in 4$) are assigned to the final node to derive crisp values (*CV*) from the posterior probabilities P_k under different conditions. The utility values of the four grades are linearly defined as $U_{low} = 0$, $U_{medium} = 1/3$, $U_{high} = 2/3$ and $U_{very\ high} = 1$ within an interval $[0, 1]$. The *CV* is calculated by combining the utility values and the marginal probabilities P_k using the utility function:

$$CV = \sum_{k=1}^{4} P_k U_k \qquad (5)$$

A high *CV* means a high SOI collision risk and a low *CV* stands for low risk.

4   A real SOI collision risk case study

In this Section, the proposed risk model is applied in a real case of a ship passing through the Liverpool Burbo Bank offshore wind farm. In the case, SOI collision risks are dynamically

assessed and calculated by using the proposed BN-based risk analylsis method. The case study is detailed as follows.

4.1 Scenario description

This study selects the Liverpool Burbo Bank offshore wind farm as a real investigation case. To test the proposed risk model, information from a ship passing the OWF waters on 29th, September 2019 is collected, covering OWF information, ship dynamic information and natural environment information. The OWF information and the AIS data are collected from a ship AIS data website (available at http://www.shipfinder.com/) and nature environment information is collected from local weather and sea report on 29th, September 2019 in Liverpool (available at https://www.worldweatheronline.com/liverpool-weather-history/merseyside/gb.aspx). Information details are listed in Table 3.

Table 3 Detail information of the scenario

Issues	Detail
OWF:	
Length of the OWF (northern boundary)	6.1 nm
The direction of the northern boundary	90°
Distance between closed OWF boundary to traffic route	1.0 nm
Type of the shipping route	One-way traffic
Corner turbines locations	53°30.1 N
Northwest corner	3°22.4 W
Northeast corner	53°30.1 N 3°12.2 W
Ship:	
Latitude (starting point)	53°31.1N
Longitude (starting point)	3°30.3W
Length	142 m
Beam	24 m
Speed (starting point)	18.6 knot
Starting course (starting point)	90.0°
Natural environment	
Sea state (Douglas sea scale)	3
Wind speed (Beaufort wind scale)	4
Visibility (nm)	More than 5

Figure 4 shows the positions of the observing points to collect information related to risk factors (e.g. AIS data and navigation conditions) during the navigation around the OWF. The time interval is 5 minutes, counting 10 different observation points in total.
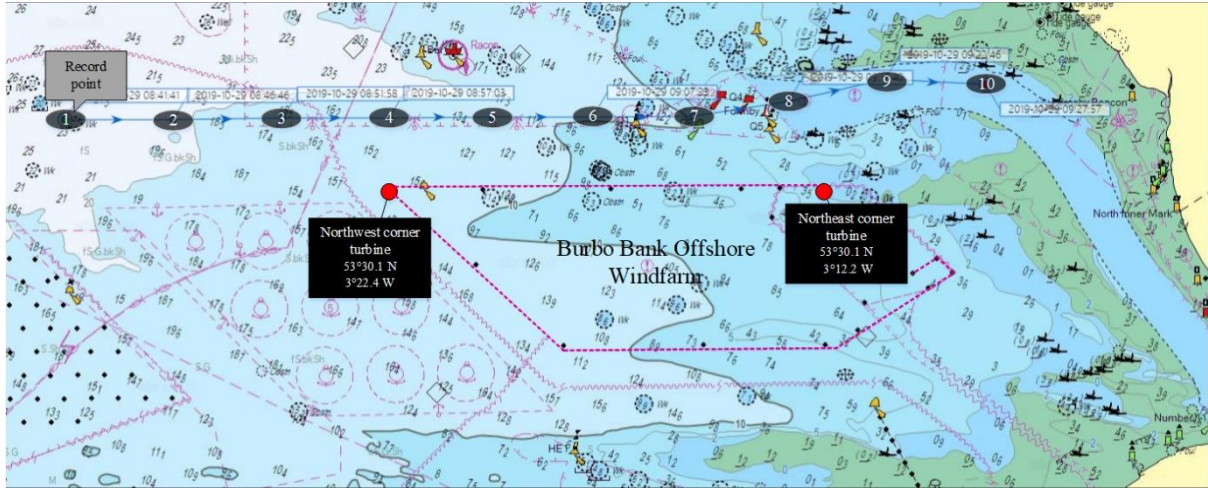

Figure 4 Ship trajectories and observation points.

4.2 Risk factor input data

The OWF's relative directions (i.e. relative bearing) are calculated using the geometrical functions (Equation 1 and 2). For example, when the ship is at Point 1, the OWF's bearing is obtained by calculating the true directions for the two corner turbines at first, then computing their relative directions. Using the relevant formulas, the true directions are: $\theta_{true}^{-} = \arctan\left(\frac{D_h}{D_v+l}\right) \times \frac{180°}{\pi} = \arctan\left(\frac{0.99}{4.73+6.1}\right) \times \frac{180°}{\pi} = 95.2°$ for the turbine in the north-west corner and $\theta_{true}^{+} = \arctan\left(\frac{D_h}{D_v}\right) \times \frac{180°}{\pi} = \arctan\left(\frac{0.99}{4.73}\right) \times \frac{180°}{\pi} = 101.8°$ for the turbine in the north-east corner. Having a ship's heading of 90.0°, the relative bearing of the OWF becomes: $\sigma_{relative}^{-} = 5.2°$ and $\sigma_{relative}^{+} = 11.8°$. Similarly, other results are calculated and given in Table 4

Table 4 Detail information for the 10 points

Point	Time	Distance (nm)	Course (degree)	Speed (knots)	Relative Bearing (degree)
1	0841	4.75	90.0	18.6	5.2, 11.8
2	0846	3.30	89.0	18.0	7.1, 17.4
3	0851	1.88	90.0	18.0	7.4, 27.4
4	0856	1.00	90.0	17.6	9.2, 85.3
5	0901	1.00	90.0	16.8	11.8, 143.3

6	0906	1.00	90.0	16.8	16.4, 159.7
7	0911	1.00	81.0	16.4	38.3, 175.3
8	0916	1.20	77.0	16.1	83.5, 180.4
9	0921	1.72	93.0	17.3	118.1, 164.2
10	0926	2.79	124.0	16.1	114.2, 135.8

It should be noted that OWFs are groups of fixed units and relative bearing of the OWF contains a far point σ^- and a near point σ^+. The belief degree of relative bearing can be obtained by computing the overlapped ranges between the interval $[\sigma^-, \sigma^+]$ and the interval of threshold values. For example, in Point 4, the relative bearing of the OWF is $[\sigma^- = 9.2, \sigma^+ = 85.3]$, which falling in three states of "*very high*" $(-22.5\sim +22.5)$, "*high*" $(+22.5\sim +45)$ and "*medium*" $(+45\sim +90)$, thus the overlapped proportions 4 are (0.29 (very high), 1 (high), 0.90 (medium)), by normalised the result, converted input of Point 4 are $BD_{VH} = \frac{0.29}{0.29+1+0.89} = 0.13, BD_H = 0.46, BD_M = 0.41$. Using Function 3 and 4, all the collected information is transformed and the converted results are shown in Appendix A.

4.3 Use the rule-based BN SOI collision risk model to conduct a collision risk analysis

The BN evaluates the ship's collision risk in each point by inputting the observed real dynamic data into eight root nodes. In this process, a Bayesian-based software (i.e. GeNIe) is employed to simplify the complex calculation procedures.

The following is an example of evaluating the collision risk. The observed data of Point 1 in Appendix A are introduced into the BN by locking the nodes as *{Speed=(1.00(VH)), Passing distance=(0.98(L), Ship type=(1.00(M)), Relative Bearing=(1.00(VH)), Sea state=(1.00,(M)), Wind =(0.67(M), 0.33(H)),Visibility=(1.00,(L)), Day/Night =(1.00,(D))}*. As a result, the software calculates the collision risk for Point 1 and describes it with an assignment for the final node (i.e. collision risk) as *(0.42(low risk), 0.25(medium risk), 0.02(high), 0.30(very high))*.

Figure 5 Collision risk for Position 1

In a similar way, the risk assignments for the other 9 points are obtained and presented in Table 5.

Table 5 Collision risk assignments for all the points

Point No.	Collision risk			
	Low	Medium	High	Very High
1	0.43	0.25	0.02	0.30
2	0.39	0.29	0.02	0.30
3	0.13	0.52	0.06	0.29
4	0.13	0.35	0.42	0.10
5	0.18	0.33	0.38	0.11
6	0.20	0.32	0.37	0.10
7	0.23	0.33	0.37	0.08
8	0.28	0.38	0.26	0.08
9	0.33	0.49	0.10	0.08
10	0.46	0.44	0.02	0.08

4.4 Calculating the crisp values to prioritise the collision risk

Using Equation 5, *CVs* for the points are calculated. For example, the *CV* for Point 1 is calculated as:

$$CV_1 = 0.43 \times 0 + 0.25 \times 0.33 + 0.02 \times 0.67 + 0.3 \times 1 = 0.40$$

Similarly, the *CVs* of the other 9 points are also calculated. The obtained *CVs* and risk assignments are presented in Figure 6 to illustrate the risk variations under different conditions.
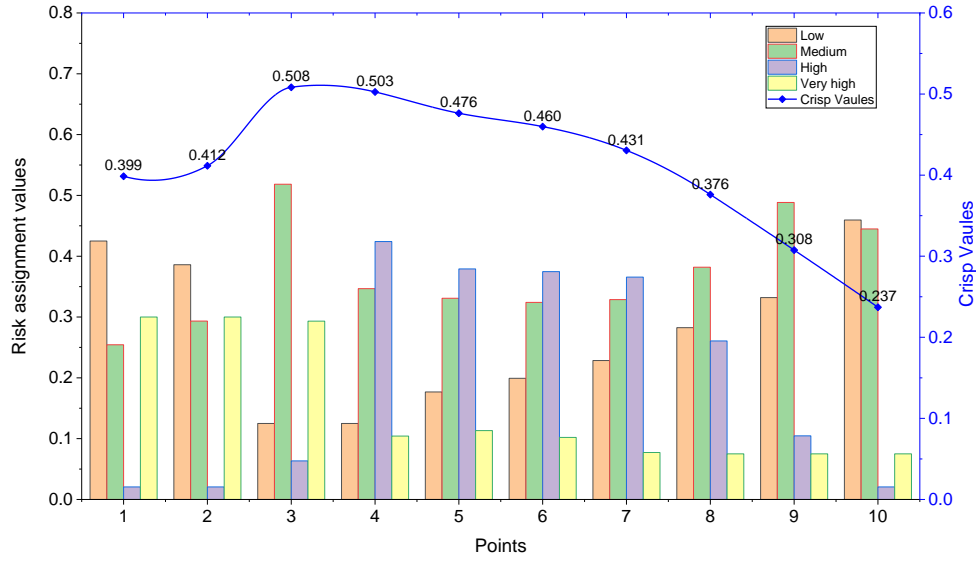
Figure 6 Collision risk under different points

5   Discussion on implications

The case study results are discussed in this section. To validate the the BN model, the obtained case results are compared with the risk calculations from a well-established collision model. Moreover, a sensitivity analysis is carried out to identify the important risk factors and critical scenarios in SOI collisions.

5.1 Case study result analysis

Section 4 analyses a real case of a ship passing through the water areas close to the Burbo Bank OWF. The collision risks under different positions are evaluated using the proposed rule-based BN model. The results reveal that during the period from Point 1 (time at 0841) to Point 3 (time on 0851), the collision risk (i.e. *CVs*) increases from 0.399 to 0.508. After the ship enters the waters close to the OWF (i.e. Point 4 to Point 8), the risk remains at a high level but slightly decreases from 0.508 to 0.376. The collision risk significantly falls after the ship passes Point 8 and finally drops to the lowest risk point (0.237) when it comes to point 10.

From the presented results, Point 3 of a ship passing the close turbine is identified as the riskiest point during its voyage, explaining that ships should pay special attention to avoid collisions when approaching the water close to OWFs. Additionally, the risk model can be repeatedly used to calculate a threshold CV value when real incident/accident reports become available. The verified setting of such a threshold is able to assist both ship owners and maritime safety administrations to take proactive control measures to reduce SOI collision risk by predicting SOI collision risk of each ship passing the waters in advance.

Meanwhile, as the impact magnitude of each risk factor is rapidly changing during the whole process of navigation, a deep analysis is required by calculating the *CVs* for each risk factor under different points of the ship trajectory. The *CVs* associated with different risk factors are calculated and the results are given in Figure 7.
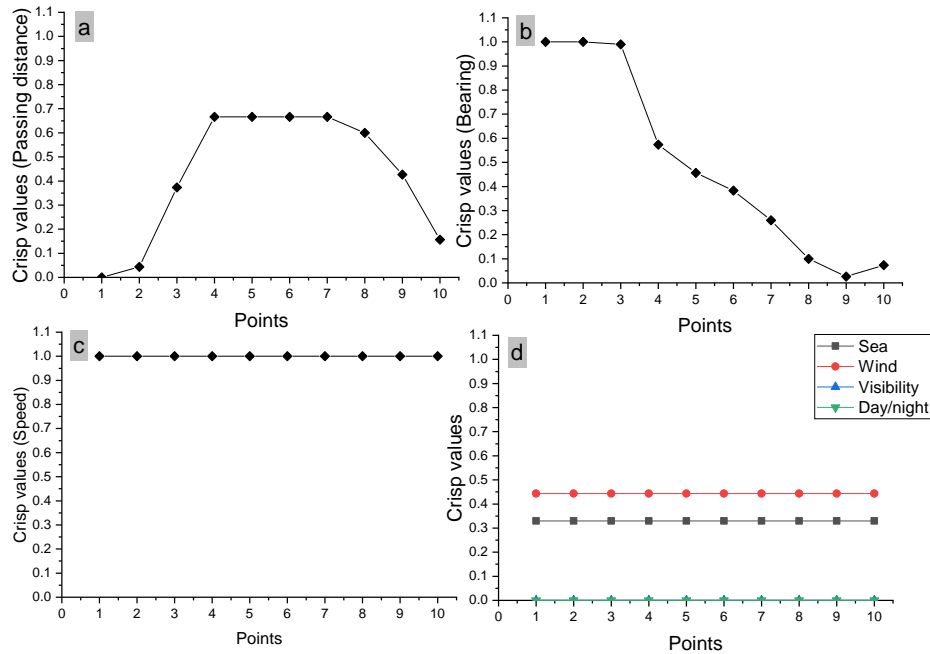

Figure 7 Crisp values for the risk factors under different points

Figure 7a reports the impact magnitude variations of the Passing distance (*D*). It contributes to a low effect magnitude (*CV*=0) when the *D* is 4.73 nm at the beginning of the passage, and rapidly increases to a high value at Point 4 ($D = 1\ nm$). The impact magnitudes of *D* remain at the value until coming to Point 8 and whereafter fall to 0.16 in the end. It concludes that the ship passes the OWF with a relative high-risk distance. Although the distances satisfy the recommendation of MGN 543 in which the ship passing distances should not be less than 0.5 nm, the ship should take extra collision avoidance measures to reduce the risk, particularly when the other risk factors (e.g. nature environment) become worse.

The effects of relative bearing σ at each point are illustrated in Figure 7b, in which Point 1 and 2 have the highest impact magnitude (*CV*=1), while point 9 obtains the lowest *CV* (0.027). From Point 1 to Point 3, corresponding to the reductions of D_h and D_v, the CVs falls from 1.00 to 0.99, indicating the slight decrease in the effects of the σ. When the ship retains its course on 90° to pass the OWF, the effects of the σ drop to the lowest value of 0.027 at Point 9.

Moreover, Figure 7c shows the effects of speed V in this scenario remain at the highest level throughout the whole trajectory. Although the ship takes deceleration when entering the waters (from 18.6 knots to 16.1 knots), its average speed (17.1 knots) is far higher than average passing speeds of 7.96 knots (Yu et al, 2020a).

Four risk factors referring to natural environments are analysed in Figure 7d. The impact magnitude of wind is evaluated as CV_W=0.443, following by sea state (CV_S=0.33), visibility (CV_{Vis} =0) and day/night time ($CV_{D/N}$=0).

The results in Figure 7 identifying the distance and the relative bearing are two important factors affecting the collision risk specific to a ship sailing within the waters close to OWFs. To mitigate the effects from distance, ships should take rational collision avoidance measures when approaching OWFs and keep safe distances subject to their navigation conditions. The relative bearing shows high effects at the beginning of the passage, thus it is defined as the main risk factor before entering into the waters close to OWFs. In addition, the ship speed shows high effects during the whole period of the scenario. Consequently, the importance of risk factors is prioritised under different stages. Speed, relative bearing and distance are three important risk factors needed to be taken seriously when the ship approaching and navigating around OWFs. After the ship approaches towards the end of the passage, high speed, close distance and very strong wind may lead to high risk.

As the BN has revealed significant real implications, it has been applied by local maritime administers to develop an offshore wind farm ship monitoring platform. As a result, the model provides effective solutions to local maritime traffic management to quickly understand the risk of ships in the waters as its practical contribution.

5.2 Model comparison and validation

To validate the new model, the scenario in this study is evaluated and the result is benchmarked by an established model proposed by Wu et al. (2018) using FLA. The reasons of selecting this research as the comparison in this study are multifaced, including 1) In terms of comparative analysis between the results from this model and an SOI risk model, we found that some SOI collision models (e.g. COLLIDE model) are not applicable to individual ship risk analysis. 2) Wu et al. (2018) conducted a ship collision risk with a static objective, presenting similar characteristics; 3) the RIFs used in both models are similar, providing the possibility for data duplication; 4) the fuzzy logic used in the paper is relatively easy to reconstructed (e.g. the essential information is provided in the paper) without the need to know much details compared

to other BN based ship collision risk models (in which the full CPTs may not necessarily be available). It makes a like-to-like comparison possible.

Both the results from the new proposed model (i.e. Rule-based BN model) and FLA based model are given in Figure 8.
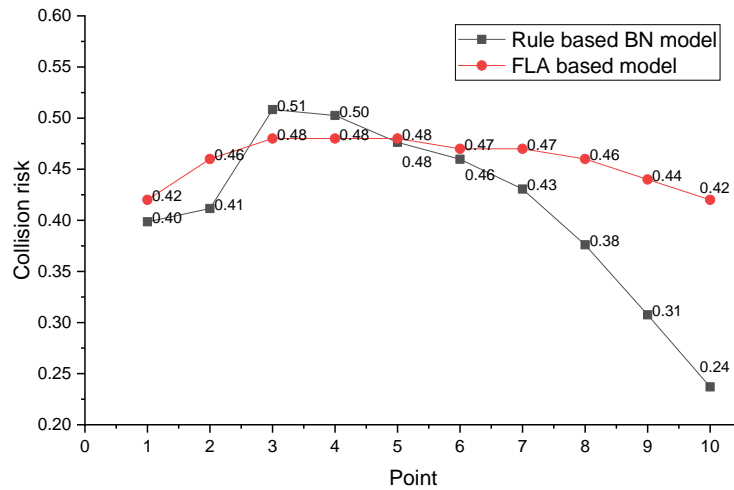

Figure 8 Correlation analysis of the risk values obtained with *rule-based BN* and *FLA* model

Figure 8 shows that the results from two models keep a great harmony in the trend of collision risk changes, indicating that the proposed model is reliable to evaluate the SOI collision risk. Meanwhile, from a generic viewpoint, there is a good correlation identified between the hybrid approach using BN and FLA with an individual approach.

Compared to the FLA model, the new BN model has an advantage in 1) the result is sensitive to the minor risk input change compare to the FLA-based model. In other words, the BN-based model enables the real-time evaluation and distinguish small collision risk changes that the FLA model fails to achieve due to its inherent incapability; 2) the BN-based model is more efficient in terms of fast computing due to the high maturity of software compared to the FLA model. The user-friendly interface helps facilitate its applications in the real world. For example, Point 3 is identified as the riskiest point using the new model whereas its risk value has increased from 0.40 to 0.51 but the same point in the FLA-based model shows no difference with its neighbours, indicating the risk of collision between Point 3, 4 and 5 is the same. It means that the results are not sensitive to the minor changes associated with Points 3, 4 and 5. Meanwhile, after ship leaving the OWF, the BN shows a significant drop on risk value (from 0.38 to 0.24) but the FLA-based model remains in a medium risk level (from 0.46 to 0.42), which shows the BN model can better reflect the risk change in the real world.

5.3 Sensitivity analysis

In this section, the sensitivity of the used variables in the model is calculated and ranked by using information entropy methods. Since the objective of this study is to investigate the importance of variables in the collision risk, we lock the node of collision risk as the target node and calculate the entropy value of variables. A higher entropy reduction value between the target and variables reveals higher importance and vice versa.

Table 6 Entropy values of variables

Nodes	Entropy Values	Relevant important rate	Categories	Rank
Passing distance	0.3	-	Ship condition	1
Relative bearing	0.225	75%	Ship condition	2
Ship type	0.15	50%	Ship condition	3
Speed	0.075	25%	Ship condition	4
Day/night	0.063	21%	Natural environment	5
Visibility	0.027	9%	Natural environment	6
Wind	0.021	7%	Natural environment	7
Sea state	0.021	7%	Natural environment	8

Table 6 reports the calculation result of the entropy value for each variable. The passing distance associates with the highest value of 0.3 thus is defined as the key variable in the SOI collision risk. It is followed by the variables of relative bearing, ship type, speed, day/night, visibility, wind and sea state in an importance decreasing order. In official offshore navigation recommendations (e.g. MGN 543), it is suggested that ship routes should keep a clear and enough distance from installations to ensure safety. The sensitivity analysis result is in line with this recommendation, partially aiding the model validation.

Meanwhile, the essential navigational condition that has the highest collision risk in offshore waters is identified. For this purpose, every scenario needs to be tested by using the BN and using the incremental update method. As it is time-consuming and hard to input manually, the scenarios have been simulated through the GeNIe software and the results are given in Figure 9.
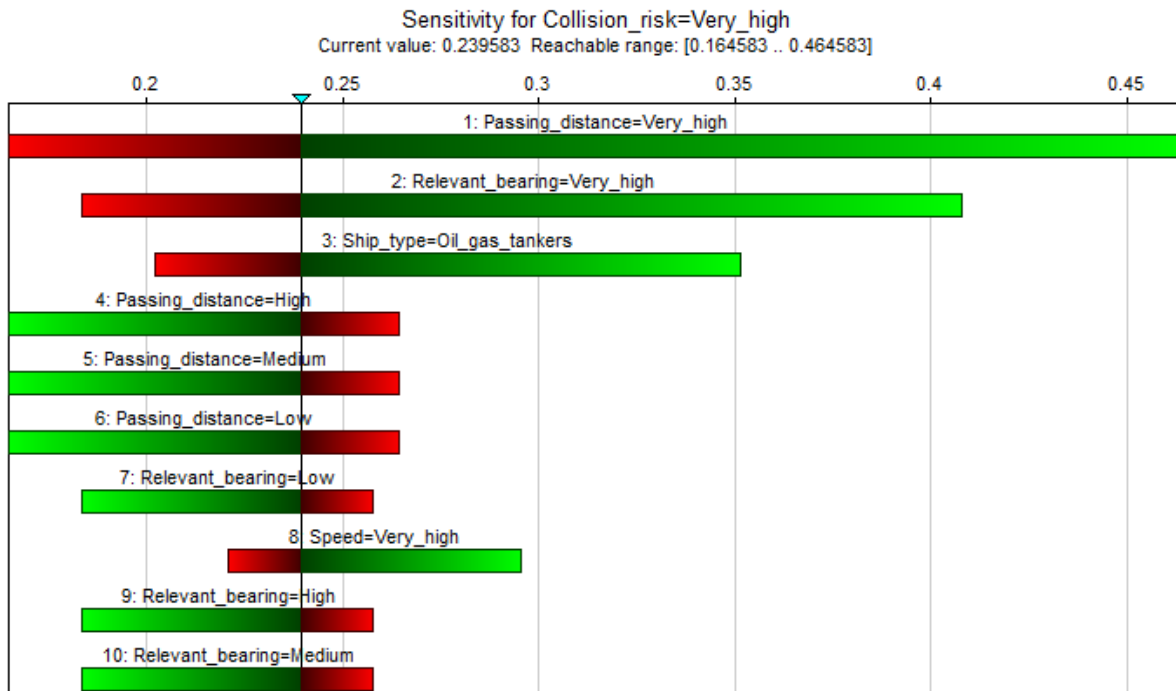
Figure 9 Sensitivity results

In Figure 9, the most critical situation leading to the collision risk can be determined, it is an oil and gas tankers passing OWF waters with a relative bearing between ± 22.5 (relative bearing=very high) and with the distance less than 0.5 nm (passing distance=very high).

It is deemed as a very useful implication in practice. As the collision between tanker and installations can cause a catastrophic consequence, the scenarios concerning tankers passing with a small distance require high safety attentions and proactive preventative measures accordingly.

5.4 Model limitations

The intended use of the proposed risk model is as an anti-collision decision aid in real-time vessel operations and shore-based vessel monitoring (e.g. VTS monitoring). The model could enhance situational awareness by providing dynamic risk values to avoid potential SOI collisions. Meanwhile, the model can be considered as a sufficient tool to simulate the risk scenarios, thus primarily an aid to support stakeholders to develop safety standards (e.g. safety distance, safe speed, etc.). Finally, although the data in the case is for passing ships when the model is applied for service ships, the CPT in the BN can be updated to better reflect the investigated content, so that given the BN's ability on CPT update to reflect the newly collected evidence. The practical value of the generic model can be emphasised by testing different

collision risk scenarios in which different types of ships and offshore installations are presented in future.

Although the model demonstrates its advantages to assess the SOI model, some limitations were found. The major restriction of the model is that the lacking relationships between relative bearing and distance, so that leads to a consequence that the risk values remain in a low level when the ship has already passed the OWF (i.e. Point 9 and 10). The limitation can be overcome by considering the safety distance under difference encounter positions (e.g. Tam and Bucknall, 2010; Goerlandt et al., 2015; Mehdi et al., 2019). For instance, using 'traditional methods' to categorise the positions of the obstacles and changing the safety distance threshold values between ownship and target ships/obstacles under different encounter situations (Tam and Bucknall, 2010); or evaluate the risk by calculating the overleap areas (i.e. manoeuvring envelope) between ownship and obstacles and between two ship (Mehdi et al., 2019).

As the ship navigation is a complex system that contains numerous impact factors (e.g. ship manoeuvres ability, human experience, and machinery/engineering system reliability, etc), the further studies related to SOI collision should be investigated to test the impct of the other (excluded) RIFs on the SOI collision risk model. The exclusion of these RIFs in this work is twofold. One is the expert survey results reveal that the values asoicate with such RIFs are unlike to significantly change during the short period of an individual ship passing an offshore object. The other is the probabilistic data is often unavailable, even the use of subjective judgement to support. For instance, the expert panel confirmed that it is extremely difficult for them to evluate human performance on an individual ship, which is highly dynamic and context demanded. The existing work on modelling human factors in ship/SOI collisions is conducted from a macro perspective. In the meantime, the expert survey in this work suggests that human related factors on invidual ships can be analysed using advanced psychological techniques (e.g. functional near-infrared spectroscopy technologies (fNIRs) (Fan et al., 2020)). A novel BN model can then be developed to evaluate SOI collision risk by considering ship manoeuvres differences. Furthermore, as the model uses expert judgements to develop the CPTs, despite the raw data showing a high level consistency, the subjective prior probability data could be further verified by the incorporation of more experts' judgements and model sensitivity analysis to avoid possible subjective bias. At last, although the model is validated through face validate and comparison, it still needs applications onboard ship to further test the model.

6 Conclusion

This paper develops a generic SOI collision risk model that can facilitate the evaluation of the SOI collision risk to support risk-informed navigational planning. By using a hybrid risk modelling approach, the mechanism of SOI collision is geometrically discussed to identify the risk factors from navigational/natural environments. After inserting the converted risk input data into a rule-based BN, the SOI collision risk is calculated.

The new SOI collision model is tested in a real scenario of a ship passing the Liverpool Burbo Bank OWFs. The model is used to evaluate the ship collision risk under different ship positions and the important risk factors are identified under different conditions to guide collision avoidance. Moreover, the new model is validated by a benchmark with an established model, the comparative analysis also demonstrates the new model has an advantage of having a more sensitive risk result, which better reflects the reality. Consequently, the application of the new SOI collision risk model demonstrates its ability to conduct dynamic SOI collision risk evaluations, which can be used either as a standalone tool or an integrated approach to support the delveopment of a decision support system in which the anti-collision measures can be tested to ensure they are cost-effective. Hence, the model can be further applied to support collision avoidance decision making systems for ships passing through offshore waters. Furthermore, the case study analysis and results further provide useful information for safety analysts and designers of OWF to conduct proactive risk management.

References

Ahn, J.H., Rhee, K.P., You, Y.J., 2012. A study on the collision avoidance of a ship using neural networks and fuzzy logic. Appl. Ocean Res. 37, 162–173. https://doi.org/10.1016/j.apor.2012.05.008

Burmeister, H.C., Bruhn, W.C., Walther, L., 2015. Interaction of harsh weather operation and collision avoidance in autonomous navigation. Int. J. Mar. Navig. Saf. Sea Transport. 9, 31–40.

Chen, P., Huang, Y., Mou, J., Van Gelder, P.H.A.J.M., 2019. Probabilistic risk analysis for ship-ship collision: State-of-the-art. Saf. Sci. 117, 108–122. https://doi.org/10.1016/j.ssci.2019.04.014

Cho, Y., Han, J., Kim, J., Lee, P. and Park, S.B., 2019. Experimental validation of a velocity obstacle

based collision avoidance algorithm for unmanned surface vehicles. IFAC-Papers On Line. 52(21), 329-334.

Coldwell, T.G., 1983. Marine traffic behaviour in restricted waters. J. Navig. 36, 431–444.

Daley, J., 2013. Mumbai high north platform disaster. Coast. Ocean Eng. Undergrad. Student Forum 1–8.

Dai, L., Ehlers, S., Rausand, M. and Utne, I.B., 2013. Risk of collision between service vessels and offshore wind turbines. Reliab. Eng. Syst. Saf, 109, 18-31.

Fan, C., Wróbel, K., Montewka, J., Gil, M., Wan, C. and Zhang, D., 2020. A framework to identify factors influencing navigational risk for Maritime Autonomous Surface Ships. Ocean Eng. 202, 107188.

Fiskin, R., Nasiboglu, E. and Yardimci, M.O., 2020. A knowledge-based framework for two-dimensional (2D) asymmetrical polygonal ship domain. Ocean Eng. 202, 107187.

Gang, L., Wang, Y., Sun, Y., Zhou, L., Zhang, M., 2016. Estimation of vessel collision risk index based on support vector machine. Adv. Mech. Eng. 8, 1–10. https://doi.org/10.1177/1687814016671250

Gil, M., Wróbel, K., Montewka, J., Goerlandt, F., 2020a. A bibliometric analysis and systematic review of shipboard Decision Support Systems for accident prevention. Saf. Sci. 128, 104717.

Gil M, Montewka J, Krata P, Hinz T, Hirdaris S., 2020b. Determination of the dynamic critical maneuvering area in an encounter between two vessels: Operation with negligible environmental disruption. Ocean Eng. 213:107709.

Goerlandt, F., Montewka, J., 2015. Maritime transportation risk analysis: Review and analysis in light of some foundational issues. Reliab. Eng. Syst. Saf. 138, 115–134. https://doi.org/10.1016/j.ress.2015.01.025

Goerlandt, F., Montewka, J., Kuzmin, V., Kujala, P., 2015. A risk-informed ship collision alert system: framework and application. Saf. Sci. 77, 182–204.

Goerlandt, F., Goite, H., Banda, O.A.V., Höglund, A., Ahonen-Rainio, P., Lensu, M., 2017. An analysis of wintertime navigational accidents in the Northern Baltic Sea. Saf. Sci. 92, 66–84.

Hansen, M.G., Jensen, T.K., Lehn-Schiøler, T., Melchild, K., Rasmussen, F.M., Ennemark, F., 2013. Empirical ship domain based on AIS data. J. Navig. 66, 931–940.

Hassel M, Utne I., Vinnem J., 2017. Allision risk analysis of offshore petroleum installations on the Norwegian Continental Shelf—an empirical study of vessel traffic patterns. WMU J. of Mar. Aff. 16, 175-95.

Hassel M, Utne I, Vinnem J., 2020. An allision risk model for passing vessels and offshore oil and gas installations on the Norwegian Continental Shelf. Proceedings of the Institution of Mechanical Engineers, Part O: Journal of Risk and Reliab. 2020, 1748006X20957481.

Hegde, J., Utne, I.B., Schjølberg, I., Thorkildsen, B., 2018. A Bayesian approach to risk modeling of autonomous subsea intervention operations. Reliab. Eng. Syst. Saf. https://doi.org/10.1016/j.ress.2018.03.019

Huang Y, Chen L, van Gelder P., 2019. Generalized velocity obstacle algorithm for preventing ship collisions at sea. Ocean Eng. 173:142-56.

İçen, D., Ersel, D., 2019. A new approach for probability calculation of fuzzy events in Bayesian Networks. Int. J. Approx. Reason. 108, 76–88. https://doi.org/10.1016/j.ijar.2019.03.004

Im, N. and Luong, T.N., 2019. Potential risk ship domain as a danger criterion for real-time ship collision risk evaluation. Ocean Eng. 194, 106610.

Kayano J, Kumagai K., 2017. Effectiveness of the OZT taking into account with the other ships' waypoints information. 2017 Joint 17th World Congress of International Fuzzy Systems Association and 9th International Conference on Soft Computing and Intelligent Systems (IFSA-SCIS): IEEE. p. 1-5.

Luo, M.F., Shin, S.H., 2016. Half-century Research Developments in Maritime Accidents: Future Directions. Accid. Anal. Prev. 123, 448–460. https://doi.org/10.1016/j.aap.2016.04.010

Ma, K.Y., Kim, J.H., Park, J.S., Lee, J.M. and Seo, J.K., 2020. A study on collision strength assessment of a jack-up rig with attendant vessel. Int. J. of Naval Arch. and Ocean Eng. 12, 241-257.

Maritime and coastguard agency., 2016. MGN 543 (M+F) Safety of Navigation: Offshore Renewable Energy Installations (OREIs) - Guidance on UK Navigational Practice, Safety and Emergency Response. Marine guidance note, Maritime and Coastguard Agency (MCA).

Mehdi, R.A., Schröder-Hinrichs, J.-U., van Overloop, J., Nilsson, H., Pålsson, J., 2018. Improving the coexistence of offshore wind farms and shipping: an international comparison of navigational risk assessment processes. WMU J. Marit. Aff. 17, 397–434.

Mehdi, R.A., Baldauf, M., Deeb, H., 2020. A dynamic risk assessment method to address safety of navigation concerns around offshore renewable energy installations. Proc. Inst. Mech. Eng. Part M J. Eng. Marit. Environ. 234, 231–244.

Mujeeb-Ahmed, M.P., Seo, J.K., Paik, J.K., 2018. Probabilistic approach for collision risk analysis of powered vessel with offshore platforms. Ocean Eng. 151, 206–221. https://doi.org/10.1016/j.oceaneng.2018.01.008

OGP, 2010. Risk Assessment Data Directory-ship/installation Collisions. International Association of Oil and Gas Producers, London, UK.

Otto, S. 2004. Offshore-Windpark Kriegers Flak. 2. Ergänzung zur Risikoanalyse. Bericht Nr. ERD2004.155, Version 1/2004-08-26. Germanischer Lloyd.

Ozturk, U., Cicek, K., 2019. Individual collision risk assessment in ship navigation: A systematic literature review. Ocean Eng. 180, 130–143. https://doi.org/10.1016/j.oceaneng.2019.03.042

Presencia, C.E., Shafiee, M., 2018. Risk analysis of maintenance ship collisions with offshore wind turbines. Int. J. Sustain. Energy 37, 576–596. https://doi.org/10.1080/14786451.2017.1327437

Perera, L.P., Carvalho, J.P. and Soares, C.G., 2011. Fuzzy logic based decision making system for collision avoidance of ocean navigation under critical collision conditions. J. of mar. sci. and tech. 16(1), 84-99.

Perera, L.P., Carvalho, J.P. and Soares, C.G., 2012. Intelligent ocean navigation and fuzzy-Bayesian decision/action formulation. IEEE J. of Oceanic Eng. 37(2), 204-219.

Perera, L.P., Guedes Soares, C., 2015. Collision risk detection and quantification in ship navigation with integrated bridge systems. Ocean Eng. 109, 344–354.

Povel D., 2006. Collision risk analysis for offshore structures and offshore wind farms. International Conference on Offshore Mechanics and Arctic Engineering. 653-61.

Safetec, 2002. Gunfleet Sands Wind Farm. Collision Risk Assessment. Report prepared by Safetec UK Ltd for Enron Wind Gunfleet Ltd. Main report, Doc. No.: 20-268-2550-1471 Rev 01, February 2002.

SAFESHIP, 2005. Reduction of Ship Collision Risks for Offshore Wind Farms. Collsision Frequencies. Deliverable No. 6; Version 2.0, 2005-01-27. Germanischer Lloyd AG, Maritime Research Institute Netherlands MARIN, Technical University of Denmark (section Maritime Engineering).

Shen, H., Hashimoto, H., Matsuda, A., Taniguchi, Y., Terada, D. and Guo, C., 2019. Automatic collision avoidance of multiple ships based on deep Q-learning. Appl. Ocean Res. 86, 268-288.

Szlapczynski, R., Krata, P. and Szlapczynska, J., 2018. Ship domain applied to determining distances for collision avoidance manoeuvres in give-way situations. Ocean Eng. 165, 43-54.

Tam, C., Bucknall, R., 2010. Collision risk assessment for ships. J. Mar. Sci. Technol. 15, 257–270.

Thieme, C.A., Utne, I.B., 2017. Safety performance monitoring of autonomous marine systems. Reliab. Eng. Syst. Saf. 159, 264–275.

Ung, S.-T., 2019. Evaluation of human error contribution to oil tanker collision using fault tree analysis and modified fuzzy Bayesian Network based CREAM. Ocean Eng. 179, 159–172.

Utne, I.B., Rokseth, B., Sørensen, A.J., Vinnem, J.E., 2020. Towards supervisory risk control of autonomous ships. Reliab. Eng. Syst. Saf. 196, 106757.

Vinnem J., 2007. Offshore risk assessment: principles, modeling and applications of QRA studies. Springer-Verlag, New York.

Wan, C., Yan, X., Zhang, D., Qu, Z., Yang, Z., 2019. An advanced fuzzy Bayesian-based FMEA approach for assessing maritime supply chain risk. Transp. Res. Part E Logist. Transp. Rev. 125, 222–240.

Wang, N., Meng, X., Xu, Q., Wang, Z., 2010. An intelligent spatial collision risk based on the quaternion ship domain. J. Navig. 63, 733–749.

Wang, Y., Zhang, J., Chen, X., Chu, X., Yan, X., 2013. A spatial-temporal forensic analysis for inland-water ship collisions using AIS data. Saf. Sci. 57, 187–202. https://doi.org/10.1016/j.ssci.2013.02.006.

Wang, X., Liu, Z., Cai, Y., 2017. The ship maneuverability based collision avoidance dynamic support system in close-quarters situation. Ocean Eng. 146, 486–497. https://doi.org/10.1016/j.oceaneng.2017.08.034

Wang, T., Wu, Q., Zhang, J., Wu, B. and Wang, Y., 2020. Autonomous decision-making scheme for multi-ship collision avoidance with iterative observation and inference. Ocean Eng. 197, 106873.

Woo, J. and Kim, N., 2020. Collision avoidance for an unmanned surface vehicle using deep reinforcement learning. Ocean Eng. 199, 107001.

Wu, B., Yip, T.L., Xie, L., Wang, Y., 2018. A fuzzy-MADM based approach for site selection of offshore wind farm in busy waterways in China. Ocean Eng. 168, 121–132. https://doi.org/10.1016/j.oceaneng.2018.08.065

Wu, B., Leung, T., Yan, X., Soares, C.G., 2019. Fuzzy logic based approach for ship-bridge collision alert system. Ocean Eng. 187, 106152. https://doi.org/10.1016/j.oceaneng.2019.106152

Yang, Z., Bonsall, S., Wang, J., 2008. Fuzzy rule-based Bayesian reasoning approach for prioritization of failures in FMEA. IEEE Trans. Reliab. 57, 517–528. https://doi.org/10.1109/TR.2008.928208

Yang, Z., Wang, J., Bonsall, S., Fang, Q., 2009. Use of fuzzy evidential reasoning in maritime security assessment. Risk Anal. 29, 95–120. https://doi.org/10.1111/j.1539-6924.2008.01158.x

Yang, Z., Wang, J., 2015. Use of fuzzy risk assessment in FMEA of offshore engineering systems. Ocean Eng. 95, 195–204. https://doi.org/10.1016/j.oceaneng.2014.11.037

Yu Q, Xin X, Liu K, Zhang J., 2018.Risk analysis of ships & offshore wind turbines collision: Risk evaluation and case study. Progress in Maritime Technology and Engineering: CRC Press. 484-90.

Yu Q, Liu K., 2019. An Expert Elicitation Analysis for Vessel Allision Risk Near the Offshore Wind Farm by Using Fuzzy Rule-Based Bayesian Network. TransNav, International Journal on Marine Navigation and Safety od Sea Transportation. 13-17.

Yu, Q., Liu, K., Teixeira, A.P. and Soares, C.G., 2020a. Assessment of the Influence of Offshore Wind Farms on Ship Traffic Flow Based on AIS Data. J. of Navig. 73(1), 131-148. https://doi.org/10.1017/S0373463319000444

Yu, Q., Liu, K., Chang, C.-H., Yang, Z., 2020b. Realising advanced risk assessment of vessel traffic flows near offshore wind farms. Reliab. Eng. Syst. Saf. 203, 107086. https://doi.org/https://doi.org/10.1016/j.ress.2020.107086

Zhang, L., Meng, Q., 2019. Probabilistic ship domain with applications to ship collision risk assessment. Ocean Eng. 186, 106130. https://doi.org/10.1016/j.oceaneng.2019.106130

Zhang, W., Kopca, C., Tang, J., Ma, D., Wang, Y., 2017. A Systematic Approach for Collision Risk Analysis based on AIS Data. J. Navig. 70, 1117–1132. https://doi.org/10.1017/S0373463317000212

Zhang, J., Zhang, D., Yan, X., Haugen, S., Soares, C.G., 2015. A distributed anti-collision decision support formulation in multi-ship encounter situations under COLREGs. Ocean Eng. 105, 336–348. https://doi.org/10.1016/j.oceaneng.2015.06.054

Zhang, W., Goerlandt, F., Kujala, P., Wang, Y., 2016. An advanced method for detecting possible near miss ship collisions from AIS data. Ocean Eng. 124, 141–156. https://doi.org/10.1016/j.oceaneng.2016.07.059

Zhou, Q., Wong, Y.D., Loh, H.S., Yuen, K.F., 2018. A fuzzy and Bayesian network CREAM model for human reliability analysis – The case of tanker shipping. Saf. Sci. 105, 149–157. https://doi.org/10.1016/j.ssci.2018.02.011

Zhu, X., Xu, H., Liu, J., 2001. Domain and its model based on neural networks. J. Navig. 54, 97–103.

Appendix A. Converted input data of the risk factors

Point No.	Speed	Ship types	Passing distance	Relative Bearing	Sea state	Wind	Visibility	Time
1	(1.00, VH)	(1.00, M)	(1.00, L),	(1.00,VH)	(1.0,M)	(0.67,M), (0.33,H)	(1.0,L)	(1.0,D)
2	(1.00, VH)	(1.00, M)	(0.87, L), (0.13, M)	(1.00,VH)	(1.0,M)	(0.67,M), (0.33,H)	(1.0,L)	(1.0,D)
3	(1.00, VH)	(1.00, M)	(0.88, M), (0.12, H)	(0.03,H), (0.97,VH)	(1.0,M)	(0.67,M), (0.33,H)	(1.0,L)	(1.0,D)
4	(1.00, VH)	(1.00, M)	(1.00, H)	(0.41,M), (0.46,H), (0.13,VH)	(1.0,M)	(0.67,M), (0.33,H)	(1.0,L)	(1.0,D)

5	(1.00, VH)	(1.00, M)	(1.00, H)	(0.23,L), (0.34,M),(0.26,H), (0.17,VH)	(1.0,M)	(0.67,M), (0.33,H)	(1.0,L)	(1.0,D)
6	(1.00, VH)	(1.00, M)	(1.00, H)	(0.33,L), (0.31,M),(0.24,H), (0.12,VH)	(1.0,M)	(0.67,M), (0.33,H)	(1.0,L)	(1.0,D)
7	(1.00, VH)	(1.00, M)	(1.00, H)	(0.46,L), (0.33,M),(0.21,H), (0.01,VH)	(1.0,M)	(0.67,M), (0.33,H)	(1.0,L)	(1.0,D)
8	(1.00, VH)	(1.00, M)	(0.20, M), (0.80, H)	(0.70,L), (0.30,M)	(1.0,M)	(0.67,M), (0.33,H)	(1.0,L)	(1.0,D)
9	(1.00, VH)	(1.00, M)	(0.72, M), (0.28, H)	(0.92,L), (0.08,M)	(1.0,M)	(0.67,M), (0.33,H)	(1.0,L)	(1.0,D)
10	(1.00, VH)	(1.00, M)	(0.53, L), (0.47, M)	(0.78,L), (0.22,M)	(1.0,M)	(0.67,M), (0.33,H)	(1.0,L)	(1.0,D)